*[Geochemistry, Geophysics, Geosystems]*

Supporting Information for

# [Retreat of the Great Escarpment of Madagascar from Geomorphic Analysis and Cosmogenic $^{10}$Be Concentrations ]

Y. Wang[1], S. D. Willett[1], D. Wu[2] , N. Haghipour[1], M. Christl[3]

[1]ETH Zurich, Department of Earth Sciences, Sonneggstrasse 5, 8092 Zurich, Switzerland.

[2]China Geological Survey, Shengyang Center, Huanghe North Street 280, 110034 Shenyang, China.

[3]ETH Zurich, Department of Physics, Laboratory of Ion Beam Physics, Otto-Stern-Weg 5, 8093 Zurich, Switzerland.

## Contents of this file



## Introduction

Figure S1 to S5 show the morphology of escarpment-draining rivers of major escarpment basins. The transformed $\chi$ profile is calculated by the integral of river length and normalized for the discharge (Perron and Royden, 2013) as there is a strong orographic effects of precipitation across the escarpment (Scroxton et al., 2017). Discharge is approximated by the product of drainage area and precipitation.

Table S1 presents escarpment retreat rates of Madagascar and Western Ghats of India that are corrected for various lithospheric rigidities and plateau area.

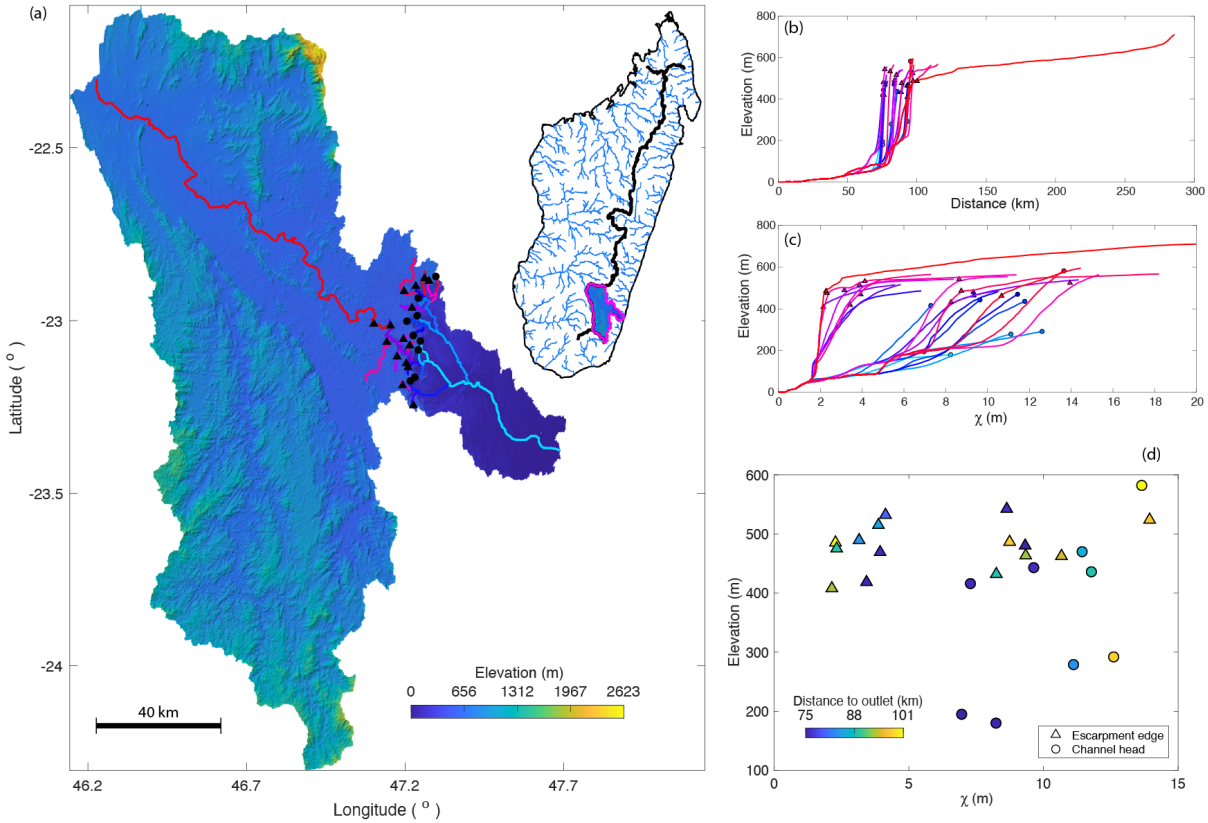


**Figure S1.** (a) SRTM digital elevation model (Jarvis et al., 2008) of the Mananara River basin in eastern Madagascar. Basin location is indicated in the inset. (b) river profiles, escarpment edges are marked with triangles and channel heads are marked with filled circles (c) transformed $\chi$-elevation profiles. (d) Position of the escarpment edge where this is identifiable as a knickzone or the channel head where there is no knickzone.

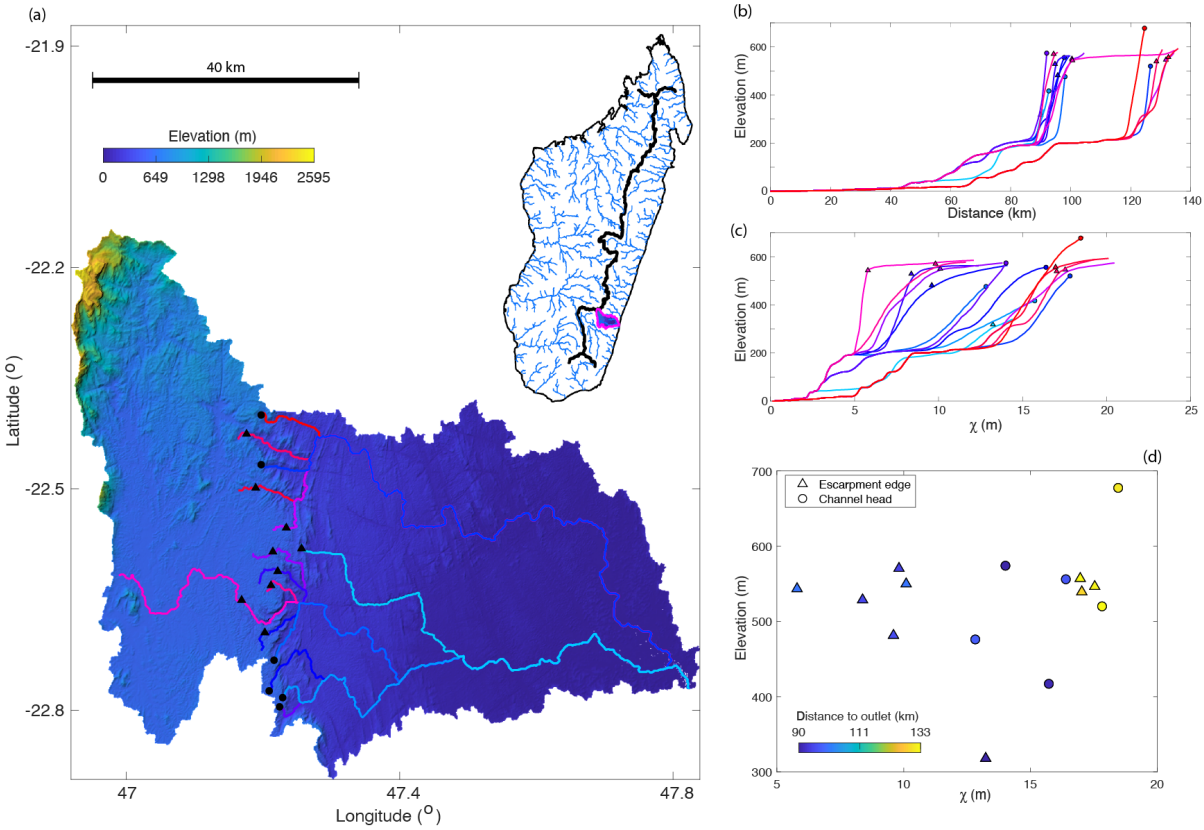


**Figure S2.** (a) SRTM digital elevation model (Jarvis et al., 2008) of an escarpment-draining basin in eastern Madagascar. Basin location is indicated in the inset. (b) river profiles, escarpment edges are marked with triangles and channel heads are marked with filled circles (c) transformed $\chi$-elevation profiles. (d) Position of the escarpment edge where this is identifiable as a knickzone or the channel head where there is no knickzone.

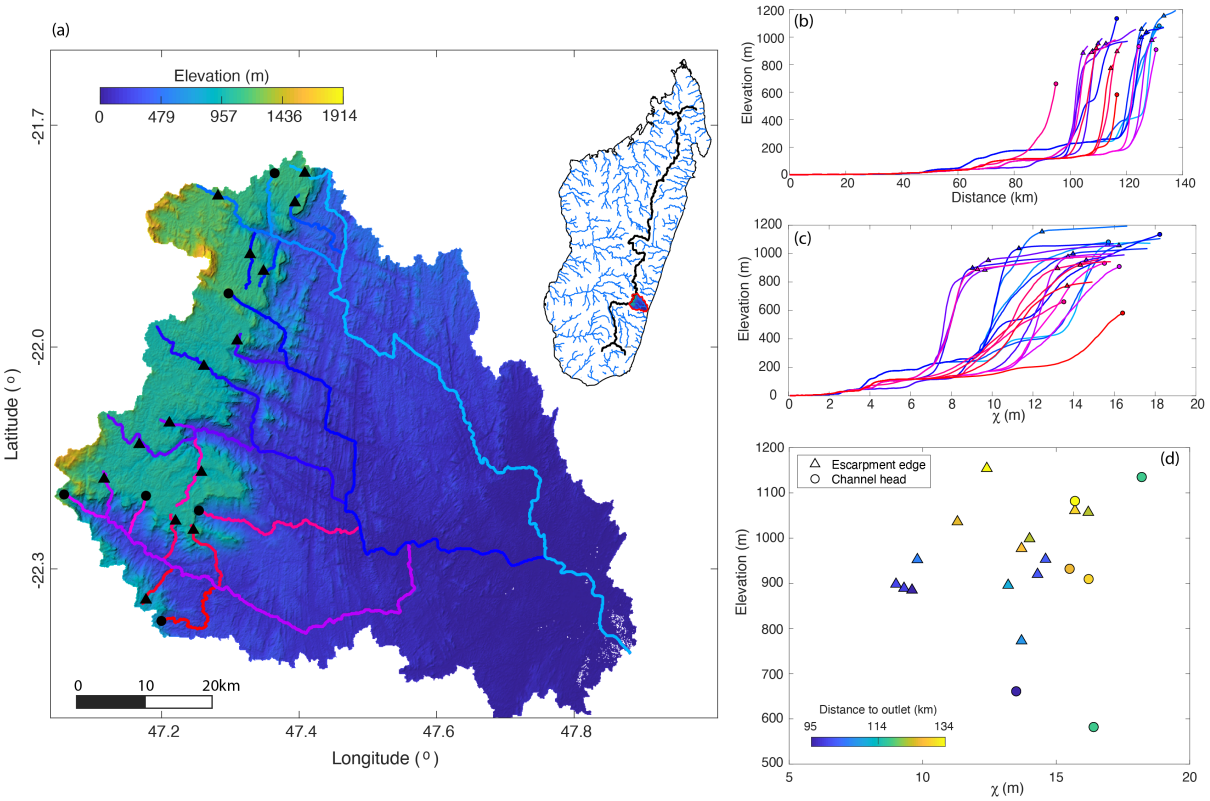


**Figure S3.** (a) SRTM digital elevation model (Jarvis et al., 2008) of an escarpment-draining basin in eastern Madagascar. Basin location is indicated in the inset. (b) river profiles, escarpment edges are marked with triangles and channel heads are marked with filled circles (c) transformed $\chi$-elevation profiles. (d) Position of the escarpment edge where this is identifiable as a knickzone or the channel head where there is no knickzone.

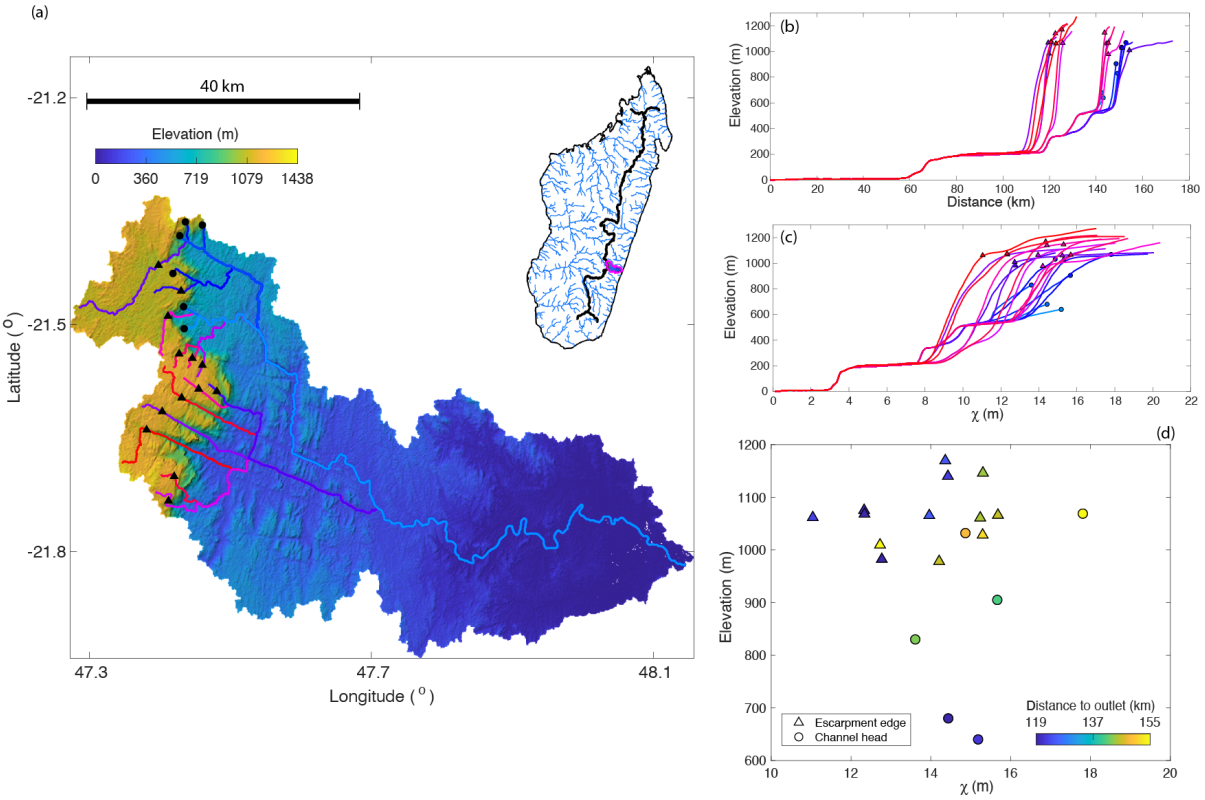

**Figure S4**. (a) SRTM digital elevation model (Jarvis et al., 2008) of an escarpment-draining basin in eastern Madagascar. Basin location is indicated in the inset. (b) river profiles, escarpment edges are marked with triangles and channel heads are marked with filled circles (c) transformed $\chi$-elevation profiles. (d) Position of the escarpment edge where this is identifiable as a knickzone or the channel head where there is no knickzone.

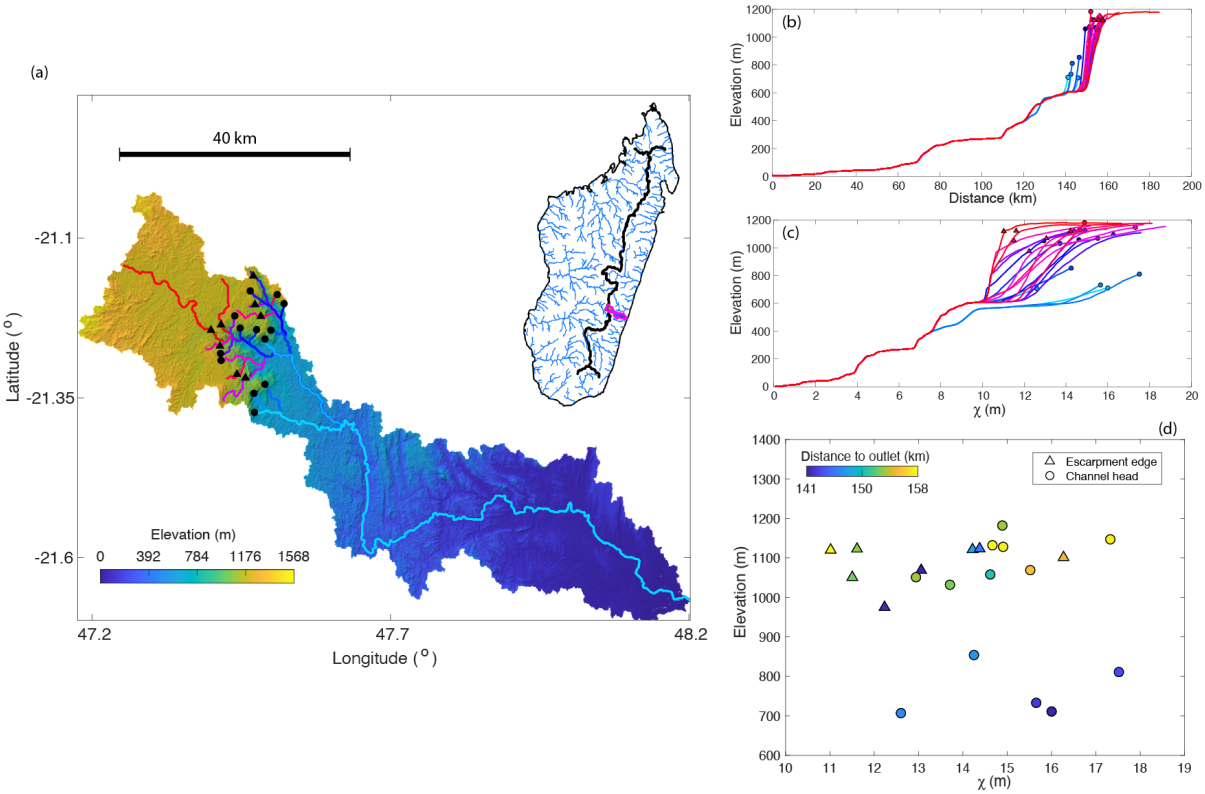


**Figure S5**. (a) SRTM digital elevation model (Jarvis et al., 2008) of an escarpment-draining basin in eastern Madagascar. Basin location is indicated in the inset. (b) river profiles, escarpment edges are marked with triangles and channel heads are marked with filled circles (c) transformed $\chi$-elevation profiles. (d) Position of the escarpment edge where this is identifiable as a knickzone or the channel head where there is no knickzone.

| Basin | [a]Flexural rebound effect $R_A$ (%) | | | Retreat rate (m/Ma) | | | $^{10}$Be reference | [d]Basin number |
|---|---|---|---|---|---|---|---|---|
| | [b]Density ratio = 0.85 | | | Corrected for both plateau area and flexural rebound | | | | |
| | [c]$Te$=5km | $Te$=10km | $Te$=50km | $Te$=5km | $Te$=10km | $Te$=50km | | |
| **Madagascar** | | | | | | | | |
| MDG_1653D2 | 22.1 | 13.9 | 4.3 | 141 | 156 | 173 | This study | 1 |
| MDG_1631B1 | 20.2 | 12.5 | 3.8 | 105 | 115 | 127 | This study | 3 |
| MDG_1609A1 | 27.0 | 17.3 | 5.4 | 195 | 221 | 253 | This study | 4 |
| MDG_1586D1 | 35.2 | 24.1 | 7.9 | 300 | 351 | 426 | This study | 5 |
| MDG_1610A1 | 42.7 | 32.8 | 11.7 | 295 | 346 | 455 | This study | 6 |
| MDG_1460C1 | 17.2 | 10.6 | 3.2 | 341 | 368 | 399 | This study | 7 |
| MDG_1405A1 | 40.6 | 29.9 | 10.3 | 699 | 825 | 1055 | This study | 9 |
| MDG_1318A2 | 37.2 | 26.1 | 8.7 | 667 | 785 | 970 | This study | 10 |
| MDG_1287B2 | 36.3 | 25.2 | 8.3 | 862 | 1012 | 1241 | This study | 11 |
| MDG_1204C1 | 34.6 | 23.5 | 7.7 | 587 | 686 | 828 | This study | 13 |
| MDG_1147D1 | 19.1 | 11.8 | 3.6 | 621 | 677 | 740 | This study | 15 |
| MDG_1176C1 | 39.2 | 28.2 | 9.5 | 821 | 970 | 1223 | This study | 14 |
| MDG_1234D1 | 43.2 | 45.3 | 25.8 | 1157 | 1115 | 1512 | This study | 12 |
| MDG_1038C1 | 41.5 | 31.1 | 10.9 | 498 | 586 | 758 | This study | 20 |
| MDG_1122C1 | 19.1 | 11.8 | 3.6 | 337 | 367 | 401 | This study | 16 |
| **Western Ghats, India** | | | | | | | | |
| SIN1440 | 21.1 | 13.1 | 4.0 | 161 | 177 | 195 | Mandal et al., 2015 | 1 |
| SIN1380 | 11.4 | 6.9 | 2.1 | 141 | 148 | 155 | Mandal et al., 2015 | 2 |
| SIN1435 | 8.1 | 4.8 | 1.5 | 177 | 184 | 190 | Mandal et al., 2015 | 3 |
| SIN1369 | 33.1 | 22.2 | 7.2 | 354 | 411 | 491 | Mandal et al., 2015 | 4 |
| SIN1368 | 30.7 | 20.2 | 6.4 | 574 | 661 | 775 | Mandal et al., 2015 | 5 |
| SIN1362 | 38.4 | 27.4 | 9.2 | 752 | 886 | 1108 | Mandal et al., 2015 | 6 |
| SIN1361 | 39.5 | 28.5 | 9.7 | 550 | 650 | 821 | Mandal et al., 2015 | 7 |
| SIN1421 | 4.8 | 2.9 | 0.9 | 307 | 313 | 319 | Mandal et al., 2015 | 8 |
| SIN1331 | 17.0 | 10.4 | 3.2 | 637 | 687 | 742 | Mandal et al., 2015 | 9 |
| SIN1332 | 23.8 | 15.0 | 4.7 | 555 | 619 | 694 | Mandal et al., 2015 | 10 |
| SIN1330 | 25.8 | 16.4 | 5.1 | 477 | 538 | 610 | Mandal et al., 2015 | 11 |
| SIN1348 | 14.7 | 8.9 | 2.7 | 288 | 308 | 329 | Mandal et al., 2015 | 12 |
| SIN1379 | 16.1 | 9.8 | 3.0 | 178 | 191 | 206 | Mandal et al., 2015 | 13 |
| SIN1416 | 6.4 | 3.8 | 1.1 | 244 | 251 | 258 | Mandal et al., 2015 | 14 |
| SIN1350 | 15.3 | 9.3 | 2.8 | 282 | 302 | 324 | Mandal et al., 2015 | 15 |
| SIN1351 | 17.2 | 10.6 | 3.2 | 349 | 377 | 408 | Mandal et al., 2015 | 16 |
| SIN1407 | 7.0 | 4.2 | 1.2 | 178 | 184 | 190 | Mandal et al., 2015 | 17 |
| SIN1433 | 8.9 | 5.4 | 1.6 | 226 | 235 | 244 | Mandal et al., 2015 | 18 |
| SIN1432 | 12.1 | 7.3 | 2.2 | 235 | 248 | 262 | Mandal et al., 2015 | 19 |
| SIN1367 | 30.4 | 20.0 | 6.3 | 327 | 375 | 440 | Mandal et al., 2015 | 20 |
| SIN1430 | 11.2 | 6.8 | 2.0 | 390 | 410 | 431 | Mandal et al., 2015 | 21 |
| SIN1427 | 6.8 | 4.1 | 1.2 | 271 | 279 | 288 | Mandal et al., 2015 | 22 |
| SIN1429 | 23.8 | 15.0 | 4.7 | 267 | 298 | 334 | Mandal et al., 2015 | 23 |
| SIN1419 | 13.1 | 7.9 | 2.4 | 429 | 455 | 482 | Mandal et al., 2015 | 24 |

**Table S1**. Flexural rebound correction for escarpment retreat rates for basins of Madagascar and Western Ghats of India. (a) the ratio of isostatically-uplifted mass removed relative to the retreat mass removal. (b) the density ratio between crust and mantle. (c) the effective elastic thickness of the lithosphere. (d) basin number on Figure 11.

## Reference


Jarvis, A., Reuter, H., Nelson, A., & Guevara, E. (2008). Hole-filled seamless SRTM data, version 4, international centre for tropical agriculture (ciat). Retrieved from http://srtm.csi.cgiar.org

Mandal, S. K., Lupker, M., Burg, J.-P., Valla, P. G., Haghipour, N., & Christl, M. (2015). Spatial variability of 10be-derived erosion rates across the southern peninsular indian escarpment: A key to landscape evolution across passive margins. Earth and Planetary Science Letters, 425 , 154-167. doi:10.1016/j.epsl.2015.05.050

Perron, J.T. and Royden, L. (2013), An integral approach to bedrock river profile analysis. Earth Surf. Process. Landforms, 38: 570-576. doi:10.1002/esp.3302

Scroxton, N., Burns, S. J., McGee, D., Hardt, B., Godfrey, L. R., Ranivoharimanana, L., & Faina, P. (2017). Hemispherically in-phase precipitation variability over the last 1700 years in a madagascar speleothem record. Quaternary Science Reviews, 164 , 25-36. doi:10.1016/j.quascirev.2017.03.017